Fuel Processing Technology 151 (2016) 50–58

Contents lists available at ScienceDirect

Fuel Processing Technology

journal homepage: www.elsevier.com/locate/fuproc

Research article

Optimizing renewable oil hydrocracking conditions for aviation bio-kerosene production

Mohit Anand [a,b], Saleem Akthar Farooqui [a], Rakesh Kumar [a], Rakesh Joshi [a], Rohit Kumar [a], Malayil Gopalan Sibi [a], Hari Singh [a], Anil Kumar Sinha [a,b,*]

[a] CSIR-Indian Institute of Petroleum, Dehradun-248 005, India
[b] Academy of Scientific and Innovative Research (AcSIR), CSIR-IIP, Dehradun-248 005, India

ARTICLE INFO

Article history:
Received 22 March 2016
Received in revised form 19 May 2016
Accepted 22 May 2016
Available online 4 June 2016

Keywords:
Hydrocracking
Triglyceride
Biofuel
Aviation fuel
Biokerosene catalyst life

ABSTRACT

In the present work we have performed a parameter study to maximize the yields of aviation bio-kerosene and renewable diesel range products obtained from the conversion of plant-oil triglycerides over Ni–W/SiO_2–Al_2O_3, hydrocracking catalyst. Specific insights and changes in reaction mechanisms, with C—O bond breaking favoured at increased pressures (>60 bar) leading to depropanation/deoxygenation, as compared to C—C bond breaking becoming favoured at reduced pressures (<60 bar) leading to formation of lower range esters and short chain glycerides, are established for the first time using analytical techniques (GC, NMR and IR). The C—C cleavage and low hydrogen partial pressures (<60 bar) led to formation of unsaturated intermediates, which promoted cyclization, aromatization and coking reactions, which increased deactivation of catalyst. High space time yield with a maximum of 240 ml/(h·$L_{catalyst}$) for <C9 products and 350 ml/(h·$L_{catalyst}$) for C9–C14 products was observed at 420 °C temperatures. Stable catalytic performance was observed until 450 h of continuous operation with 25–30% yield of aviation bio-kerosene which meets all ASTM D 7566 standards.

1. Introduction

Bio-based sources, for meeting the present transportation sector needs would not only reduce the burden and dependence on crude oil, but also help the transportations sector to reduce their carbon footprint [1,3–9]. Plant oils may either be trans-esterified to give biodiesel, which can be blended in the diesel pool and used in the engines (such as 5% or more according to European biodiesel specification, EN 14214, EN 590), or they may be hydroprocessed to produce drop–in kind of biofuels wherein there are no limits on blending as they match crude derived diesel properties. Thus, hydroprocessing route is a better option because it can use existing refineries and produces hydrocarbons very similar to the ones in petroleum oil and hence can be directly used (drop-in fuel) without any changes in the existing engines [1,10–17]. Bio-aviation kerosene combustion reduces particulate emissions (due to lower aromatics content in the fuel) as well as SOx emissions (due to lower S content in the fuel) as compared to the combustion of petroleum derived kerosene [18]. Aviation sector depends very strongly on liquid hydrocarbon fuels as compared to road transportation sector, so targeting technologies which maximize kerosene yield from bio-based sources would be more desirable as compared to diesel fuels.

Biomass derived oils containing triglyceride with 9–10 wt% oxygen, not only reduces the heating value but also leads to storage stability issues [17,19]. In literature various studies on model compounds like tristearin (glycerol tristearate C18), triolean (glycerol trioleate C18), tricaprylin (Octanoic acid triglyceride C8) and caprylic acid (octanoic acid C8) [13,16,20–22] have been carried out to predict reaction mechanisms. Various supported metals, mono-functional [20,23,24] or bi-functional [1,2,25–27] catalysts, have been used for hydrotreatment of triglycerides (to remove 'O' only) [8,17,23,24,26–29] and for hydrocracking to produce lower boiling hydrocarbons [1,2,8,24,25]. Low acidity supports like γ-Al_2O_3 or activated carbon [8,17,23,24,26–29] were used for hydrotreatment, where as moderately acidic supports such as amorphous mixed oxides like silica-alumina [1,2,8,25] or phosphate modified silica-alumina [25] or crystalline highly acidic aluminosilicate supports like zeolites [1,15,25,24] were used for hydrocracking/isomerization reactions. All these supports (acidic/non-acidic) were impregnated with active metals like Pd, Pt, Pt–Re, or sulfide NiW, NiMo, CoMo for hydrogenation/dehydrogenation ability.

Earlier studies have reported CoMo and NiMo catalysts for removing oxygen from these oxygenated feeds [7,8,17,28,30]. Very few studies have been carried out over NiW based catalyst systems which offer enhanced hydrogenation ability [2] as compared to molybdenum based catalysts (CoMo, Ni–Mo) systems. Stronger hydrogenating ability is expected to reduce the formation of waxy oligomeric products and also improves the quality of end products such as bio-aviation kerosene.

* Corresponding author at: CSIR-Indian Institute of Petroleum, Dehradun-248 005, India.
E-mail address: asinha@iip.res.in (A.K. Sinha).

http://dx.doi.org/10.1016/j.fuproc.2016.05.028
0378-3820/

Detailed understanding of process parameters such as temperature, hydrogen partial pressures and H_2/feed ratios is necessary for optimizing the yield of different products such as naphtha, kerosene and diesel, which has been targeted for the first time for NiW catalytic system. For commercial realization of these biomass-oil derived fuels specifically for aviation bio-kerosene, detailed process parameter evaluation along with catalyst life time studies have been targeted. Insights into reaction mechanism and intermediates formed were derived using IR, ^{13}C NMR studies. This would enable optimization of reaction conditions to maximize the yield of the most desirable products.

2. Experimental

Powdered and extrudates of Ni–W/SiO_2–Al_2O_3 catalyst were loaded in a fixed bed reactor (2 g of catalysts (Catalyst: SiC 1:1), catalyst bed volume 4.64 ml, bed height 3.5 cm, reactor volume 40 ml, reactor I.D. 1.3 cm and reactor length 30 cm). The catalyst was prepared by conventional impregnation of 4% NiO, 24%WO_3 over extrudates of mesoporous SiO_2–Al_2O_3 support (BET surface area = 274 m^2/g, pore volume of 0.6 ml/g, and mean pore diameter of 15 nm). The method of preparation, catalyst loading and reactor setup and sulfidation details are given elsewhere [1,30–31].

The properties of the porous catalysts like surface area, pore volume, pore size were examined at 77 K using Belsorb Max (BEL, Japan) by measuring N_2 adsorption–desorption isotherms. The total acidity of the catalyst was measured using Micrometrics 2900 chemisorption equipment equipped with a thermal conductivity detector. Ammonia was used as an adsorbent and 0.15 g sample was saturated with NH_3 at 393 K. Helium was flushed over the sample to remove any physically adsorbed NH_3. Desorption of NH_3 was then measured at a heating rate of 10 °C/min in helium flow. The surface of the catalyst was analysed using a field emission scanning electron microscope (SEM) model FEI Quanta 200 F, fitted with an Everhart-Thornley detector (ETD) for the measurement of secondary and backscattered electrons. SEM images were obtained under high vacuum mode using tungsten filament doped with lanthanum hexaboride (LaB_6) as an X-ray source, using secondary electrons with an acceleration tension of 10 or 30 kV. Energy-dispersive X-ray spectroscopy (EDX) coupled with SEM was used for elemental analysis and elemental mapping. Micromeritics 2720 equipment was used for determining metal sulfide dispersions in the sulfided catalyst by H_2-chemisorption. The catalyst sample was sulfided [1,30–31] using dimethyl disulfide (in the same way as done prior to catalytic studies), and then loaded into the Micromeritics 2720 equipments sample tube under hydrogen atmosphere. The samples was heated to 250 °C (at 2 °C/min) in H_2 (99.999%), and held for 1 h to remove any adsorbed moisture and then evacuated for 1 h at 250 °C to remove any chemisorbed hydrogen. Total uptake of hydrogen was measured by manual injection of hydrogen (1 ml injection volume, H_2:He 10:90) until it reached saturation and the total dispersion was calculated using the standard equations [32,33]. TEM images were recorded using FEI, series Tecnai G2 operating at 200 kV.

Jatropha oil (1.7% FFA (free fatty acids), 19.5% C16:0 (all saturated bonds), 7.9% C18:0 (all saturated bonds), 45.4% C18:1 (one unsaturated bond), 27.3% C18:2 (two unsaturated bond), 77.0 wt% C, 13.6 wt% H, 9.4 wt% O, 4.0 ppm S; Na: 3.2, K: 28.9, Mg: 17.3, Ca: 21.5, P: 35.6, Si: 6.4 ppmw) was processed in a catalytic fixed bed reactor from, 340–420 °C temperatures, 20–90 bar pressure and 1500–2500 NL_{gas}/L_{liquid} H_2/Feed ratios. The unconverted jatropha oil and the liquid products obtained after deoxygenation, cracking and isomerization reactions were analysed offline after separation of the water phase, using a GC (Varian 3800-GC) equipped with a FID and a TCD. Vf-5ms column (30 m × 0.25 mm, 0.25 μm) was used and internal standard (eicosane) were used for quantification. Elementar Micro-cube analyzer was used for CHNS analysis and Rudolf research analytical instrument (DDM-2911) was used for analysis of density of the liquid products. Material and elemental balance were recorded to evaluate and confirm minimal error in experimental measurements. The quantity of liquid feed and products were measured using a weighing balance with an precision of ±1 g (Pilot scale) and ±0.01 g (Micro-reactor scale). All reaction products were withdrawn after stabilization of reaction conditions in each experiment and were analysed in stabilization period until constant activity of the catalyst was observed. Products were grouped in three categories according to carbon no, <C9 carbon range liquid products were grouped as naphtha, C9–C14 carbon range products were grouped as kerosene and >C15 products (i.e. C15–C18 major products and >C18 minor products) were grouped as diesel. Space time yields (STY) was calculated as the ratio of volumetric product rate (ml/h) to the amount of catalyst (volume) used in obtaining that product.

For pilot plant evaluation, a reactor with 600 ml capacity (Xytel India) was used for catalyst life-time and regenerability studies (100 g of catalysts (Catalyst: SiC 1:1), catalyst bed volume 318 ml, bed height 45 cm). The catalytic evaluation was carried out round the clock. Type K thermocouples were used for temperature measurement both inside and outside the reactor which were calibrated to an accuracy of ±1 K. All the results were obtained under steady state conditions. The products obtained were analysed using the similar procedure as described above. The aviation bio-kerosene was analysed specifically for properties as per ASTM D 7566 and standard procedures for all methods were followed as described in "Standard Specification for Aviation Turbine Fuel Containing Synthesized Hydrocarbons" [34]. Error in experimental and measurement uncertainties was determined and is included in the final results. A standard calibration sample was analysed prior to analysis of unknown samples to determine uncertainties with respect to equipment calibration and accuracy. If a deviation of >0.1% was observed, then it was incorporated in the measured quantities. The precision and error in measurement for each ASTM method was accounted by analysing samples twice after stabilization of the equipment and they have been included with the final results. It was not possible to calculate data at very low conversions (<15%) due to practical problems in running the experiments due to wax accumulation in the reactor setup at low conversions.

3. Result and discussion

The catalyst characterization and product variation is given in the following sections.

3.1. Catalyst characterization

FE-SEM images in Fig. 1(a and b) show surface morphology of the sulfided NiW/SiO_2–Al_2O_3 catalyst wherein nanoparticles of sizes 10–20 nm were observed. TEM images (Fig. 1c and d) of the sulfided catalyst show well-dispersed densely populating NiW-S nanoslabs 2–3 nm wide and 20–80 nm long. The lattice fringes with inter-layers spacing of 0.3 nm were observed (Fig. 1d, inset). Considering the interlayer spacing of 0.3 nm, NiW-S nanoslabs would consist of approximately 7 to 10 layers.

Hydrogen chemisorption studies on sulfided catalyst showed a 30% dispersion value indicating well dispersed active metal as also observed by high resolution FE-SEM and TEM analyses. After impregnation the catalyst showed narrow pore size distribution with moderate surface area of 233 m^2/g, pore volume 0.32 ml/g, mean pore diameter of 10.2 nm and surface acidity of 0.77 mmol/g. The mesoporous catalyst surface, along with acidity combined with strong hydrogenation functionality imparted by tungsten and nickel metal sulfides were required for hydrocracking and hydrotreating of bulky triglyceride molecules into usable hydrocarbons.

3.2. Catalytic studies

It is expected that thermal reactions would be occurring, at the studied temperatures. Blind test without catalyst were performed with

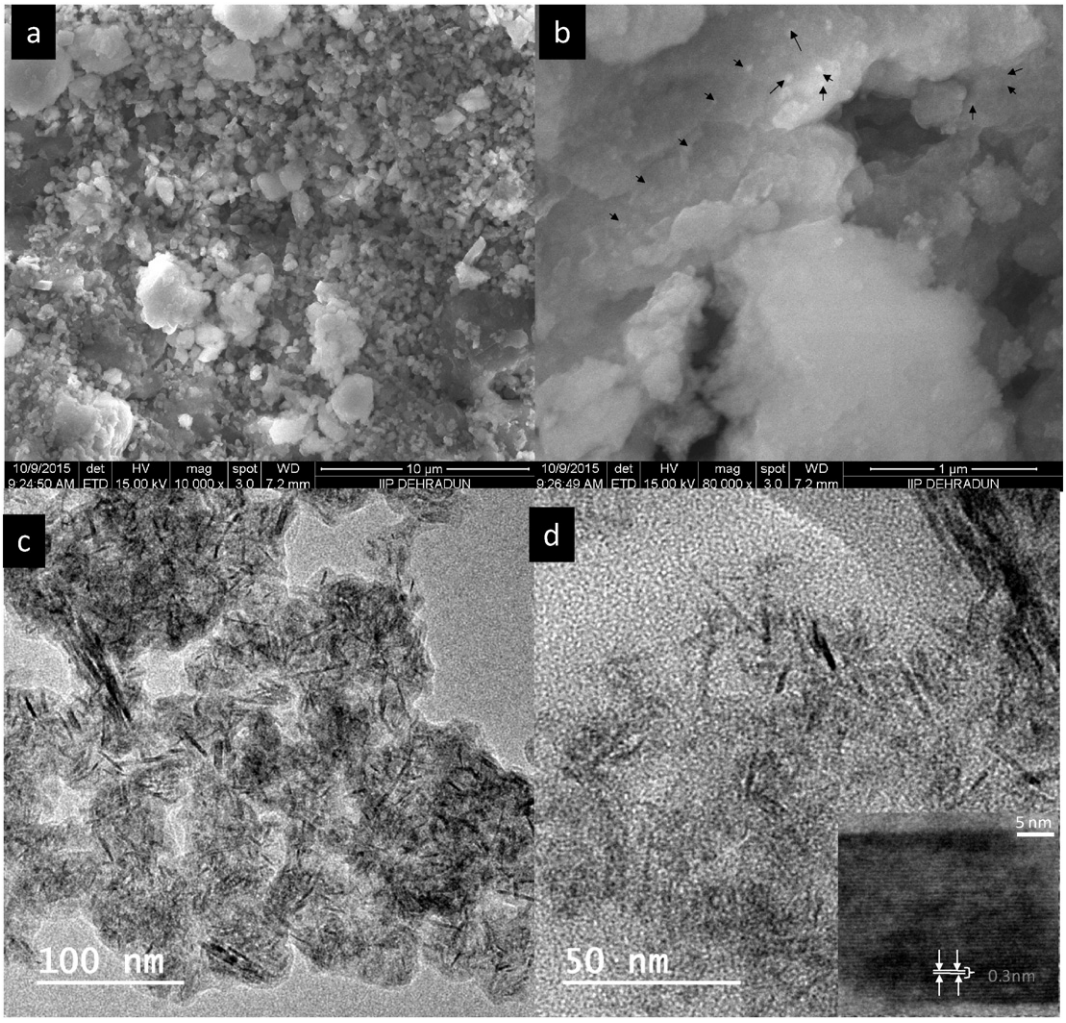

Fig. 1. FESEM (a and b) and TEM (c and d) images of sulfided catalyst.

jatropha as a feed to monitor thermal cracking of jatropha. Approximately 85–95% yield of oligomerized (>C18 range) products was obtained with similar oxygen content as in the feed. This indicates negligible deoxygenation and cracking reactions, with formation of undesirable products in the absence of catalyst.

The product patterns obtained during the hydroprocessing of triglycerides over sulfided Ni–W/SiO_2–Al_2O_3 catalyst were used for calculating the space time yields (STY) of various product groups. These STYs gave valuable insights for optimizing process conditions for different products at industrial scale.

3.2.1. Temperature and space velocity effect

Space time yield (STY) (Fig. 2) of the total products (based on triglyceride conversion) increased (almost linear increase) with an increase in temperature from 340 °C to 420 °C, at higher space velocities (9 h^{-1} and 12 h^{-1}). This was due to increasing conversion of triglycerides molecules with increase in temperature, which increased the total products yield. Whereas at lower space velocities (1 h^{-1}–6 h^{-1}) the space time yield (STY) of total products became constant beyond 360 °C temperatures, due to complete conversion of triglycerides at these conditions. The space time yield (STY) was clearly observed to increase with increasing space velocity at reaction temperatures beyond 360 °C. The conversion of triglycerides was also reduced significantly on lowering the pressures (40–20 bar) with 70% conversion at reactor pressure of 40 bar, which further decreased to 67% at 20 bar (Fig. 3). The effect of pressure on conversion of triglycerides was more significant on Ni–W system than that reported earlier on Co–Mo systems [17,30]. The comparatively lower conversion of triglycerides (70%) for Ni–W catalyst at 40 bar pressure, than that obtained over Co–Mo catalyst (91%) [30], may be attributed to the better

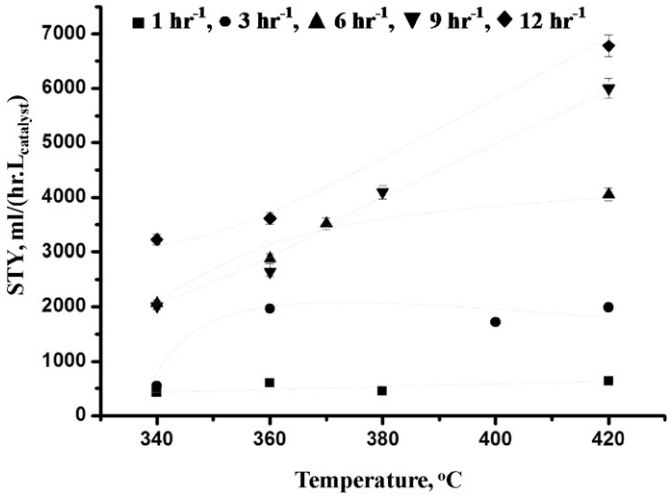

Fig. 2. Influence of temperature on the space time yield (STY) of all the products (based on Triglycerides conversion) at various space velocities (80 bar, 1500 NL_{gas}/L_{liquid}).

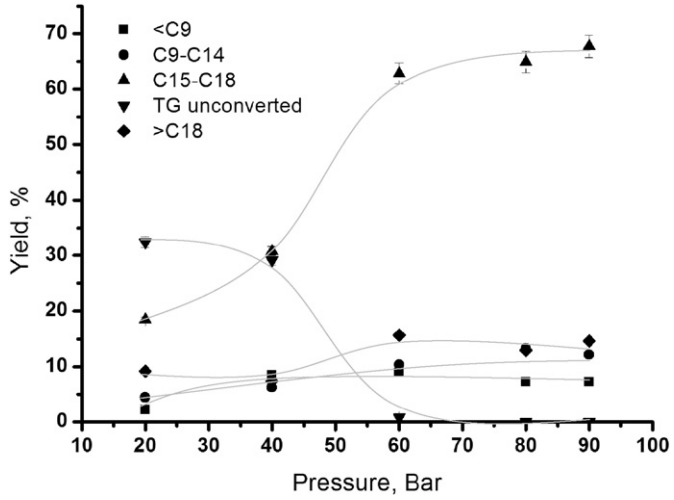

Fig. 3. Influence of pressure on yield fractions of various lumps ('TG' Triglycerides; 'Cn' hydrocarbons with carbon number 'n') (3 h^{-1}, 420 °C, 1500 NL_{gas}/L_{liquid}).

deoxygenating ability of Co–Mo at lower pressures. Co–Mo is a better hydrodesulfurization catalyst at lower pressures as compared to Ni–W catalyst, and the same appears to be true for hydrodeoxygenation reactions.

The space time yield (STY) for both <C9 (Fig. 4a) and C9–C14 (Fig. 4b) lump was very low and almost constant at approximately 5–25 ml/($h \cdot L_{catalyst}$) until 360 °C reaction temperature, indicating very low formation of cracked products at lower temperatures. The space time yield increased rapidly with increase in temperature to 420 °C and reached a maximum value of 240 ml/($h \cdot L_{catalyst}$) for <C9 products and 350 ml/($h \cdot L_{catalyst}$) for C9–C14 products with increase in temperature indicating an increase in cracked products at higher temperature, at all space velocities. There was an increase in space time yield of C15–C18 carbon-range hydrocarbon products with increase in reaction temperature from 340 °C to 360 °C at 1–6 h^{-1} space velocities (Fig. 4c). On further increasing the temperature from 360 °C to 420 °C a maxima in space time yield for C15–C18 products was observed at 1–9 h^{-1}, due to conversion of this range product into other lower carbon-range cracked hydrocarbons. On contrary at 12 h^{-1} space velocity no decrease in space time yield for these products were observed, rather a gradual increase was noted with increasing temperature. This increase in space time yield for C15–C18 products at higher space velocity (12 h^{-1}) can be correlated with the increasing conversion of triglycerides with temperature (Fig. 2) and also to reduced secondary conversion reactions at higher space velocities. This observation along with increased yield of cracked lower range hydrocarbons (<C9 and C9–C14) at higher temperatures, indicates a shift in reaction pathway from primary deoxygenation reactions to secondary cracking and isomerisation reactions along with deoxygenation reactions [30]. The space time yield (STY) of oligomeric (>C18) products was suppressed at lower space velocities (1, 3 h^{-1}), but was very high at higher space velocities, and reduced rapidly on increasing the temperature from 340 °C to 380 °C. On further increasing the temperature from 380 °C to 420 °C, slight increase in space time yield of >C18 range products was observed (at 6–12 h^{-1}) indicating that these are thermodynamically controlled products. >3000 ml/($h \cdot L_{catalyst}$) yield was observed at 12 h^{-1} space velocity which reduced to 400 ml/($h \cdot L_{catalyst}$) at 380 °C but again increased to 800 ml/($h \cdot L_{catalyst}$) at 420 °C (Fig. 4d).

These results indicated that although high space time yields were obtained for cracked lower range hydrocarbons (<C9 and C9–C14) at greater space velocities (6–12 h^{-1}) at all ranges of temperatures, these were not the optimum conditions due to increased formation of

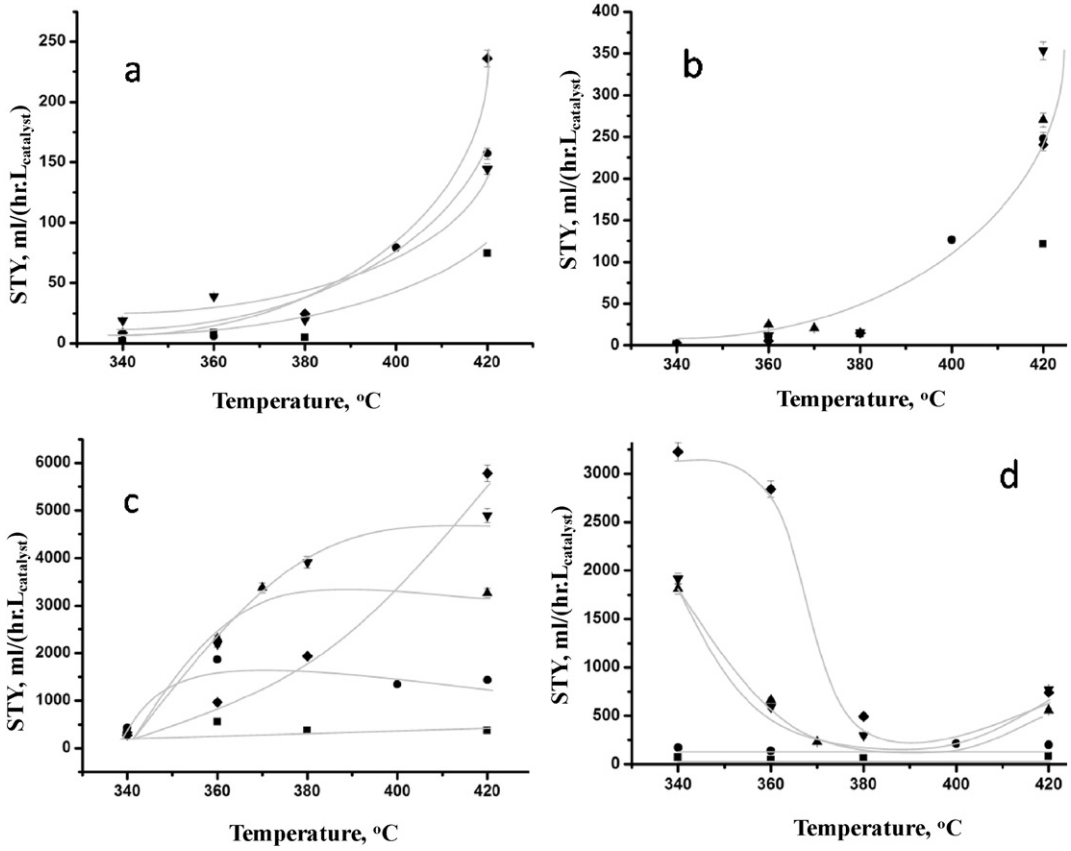

Fig. 4. Space time yield of 'Cn' hydrocarbons with carbon number 'n' (a:<C9, b: C9–C14, c: C15–C18, d: >C18) as a function of reaction temperature at different space velocities (■ 1 h^{-1}, ● 3 h^{-1}, ▲ 6 h^{-1}, ▼ 9 h^{-1}, ♦ 12 h^{-1}, 80 bar, 1500 NL_{gas}/L_{liquid}).

the side oligomeric waxy products. Lower space velocities ($1-3\ h^{-1}$) and higher temperatures (>400 °C) were required for increasing the yield of naphtha and kerosene range hydrocarbons and to minimize the diesel pool yield. If diesel was the desired product, then reduced temperatures (<380 °C) were required for minimizing the secondary cracking reactions.

3.2.2. Pressure effect

Fig. 3 shows the influence of pressure on yield fractions of various lumps at 3 h^{-1}, 420 °C and 1500 NL_{gas}/L_{liquid} H_2/feed ratio. Monotonic increase and decrease, respectively, in the yield of deoxygenation products (C15–C18 hydrocarbons) and unconverted triglycerides was observed as the pressure was increased from 20 to 80 bar (Fig. 3). There was only slight effect of pressure on the formation (yield) of >C18 products (10% at 20 bar to 12% at 90 bar), whereas there was gradual increase in the formation of naphtha and kerosene fraction at higher pressures (2% at 20 bar to 10% at 90 bar). This indicates that partial pressure of hydrogen influences the formation of cracked lower range hydrocarbons. Also some unknown oxygenated compounds were observed at lower pressures (Fig. 5), whose concentration increased from 0% at 80 bar to approximately 34% at 20 bar (Fig. 5 inset). IR (C═O stretch at 1711.8 cm^{-1} and C—O stretch at 1377.2 cm^{-1} (Fig. 6)) and ^{13}C NMR spectra (chemical shift at 180 of C═O observed at 20 bar pressure; Fig. 6) confirmed their formation. The characteristic C—O stretching vibrations [35] for unconverted triglycerides are generally observed at 1286 cm^{-1} (1150–1350 cm^{-1}) which was absent in these products. The formation of lower range esters indicated formation of short chain glycerides at lower pressures, and a shift in reaction mechanism from depropanation/deoxygenation (C—O bond cleavage, at higher pressures, >60 bar) to cracking (C—C bond cleavage, at lower pressures, <60 bar). It is anticipated that at higher pressures (>60 bar), the catalyst Ni–W/SiO_2–Al_2O_3, promoted the C—O cleavage which was driving the reaction whereas at lower pressure (<60 bar) C—C cleavage was more significant. The C—C cleavage and low hydrogen partial pressures (<60 bar) led to formation of unsaturated intermediates, which promoted cyclization and aromatization reactions (C═C aromatic stretch at 1464.3 cm^{-1} and chemical shift between 120 and 140; Fig. 6). These reactions were the precursors to coke formation reactions and hence contributed to deactivation of catalyst at lower pressures. Therefore, operation at higher pressures (>60 bar) was necessary for increased catalyst performance and enhanced catalyst life.

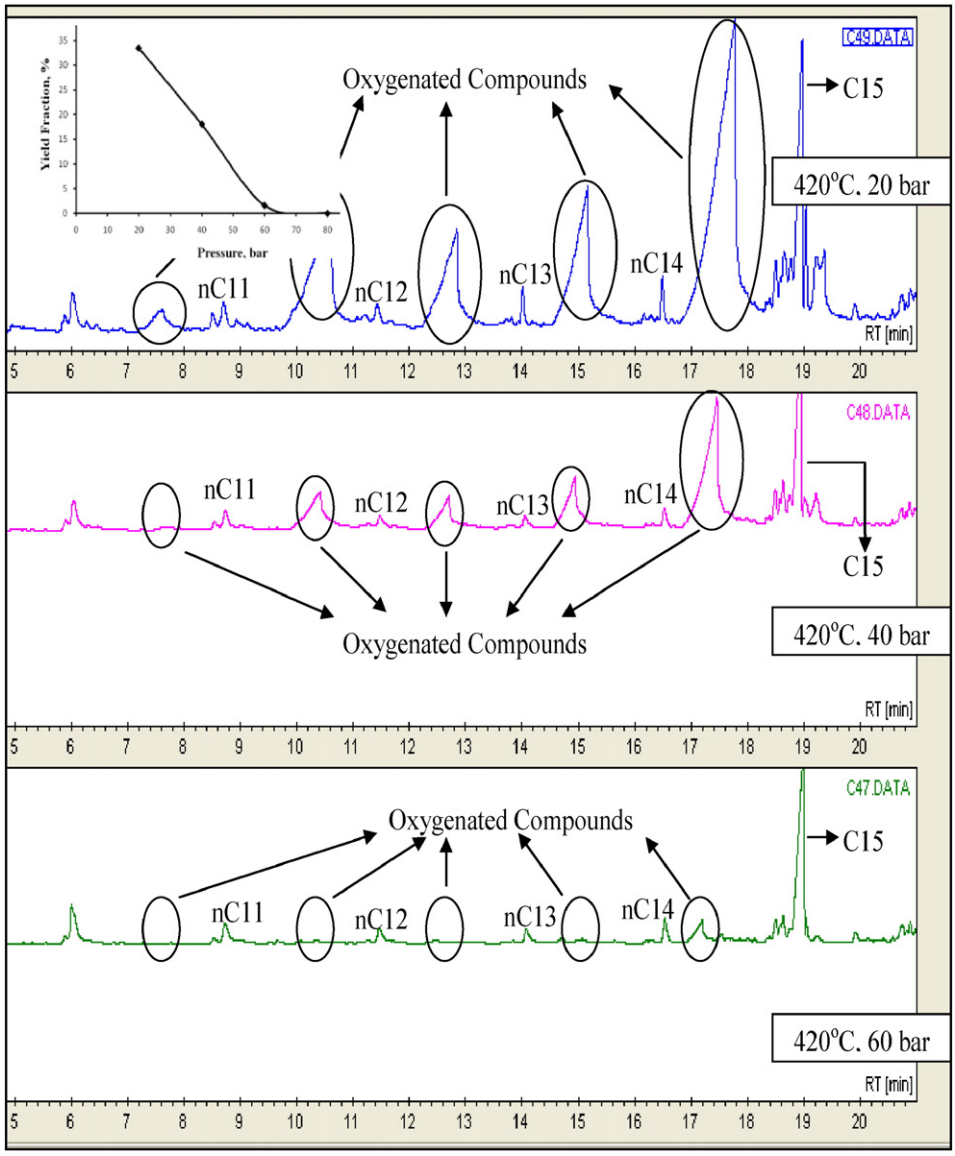

Fig. 5. Gas Chromatograms showing unknown oxygenated compounds, at varying pressures (3 h^{-1}, 420 °C, 1500 NL_{gas}/L_{liquid}); Inset: Yield fractions of cracked oxygenated products as a function of reactor pressure.

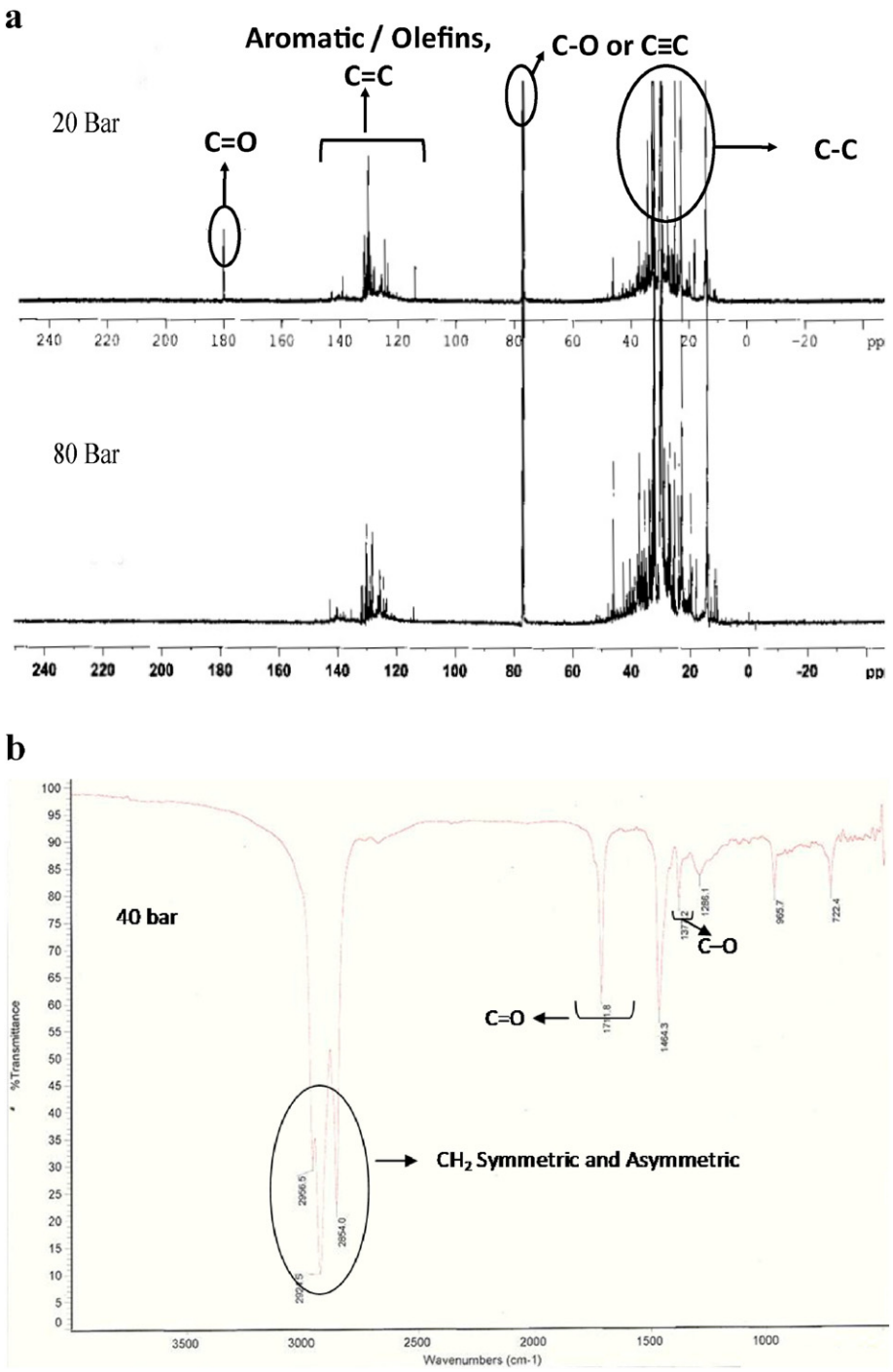

Fig. 6. C13-NMR spectra (a.) and FTIR transmittance spectra (b.) for unknown oxygenated compounds observed at 3 h^{-1}, 420 °C, 1500 NL_{gas}/L_{liquid}.

Table 1
Influence of H_2/feed ratio on yield fractions of various lumps (at 3 h^{-1}).

Temperature, °C	H_2/Feed ratio, NL_{gas}/L_{liquid}	<C9	C9–C14	C15–C18	Triglycerides unconverted	>C18
360	500	0.07	0.05	17.31	73.86	8.71
	2500	0.24	0.18	33.54	53.19	12.85
420	500	3.00	11.40	76.66	1.42	7.53
	1500	7.23	12.15	67.70	0.00	12.92
	2500	9.10	13.46	64.34	0.00	13.11

3.2.3. H_2/Feed ratio effect

Table 1 shows the influence of H_2/feed ratio on the yield fractions of various lumps (at 3 h^{-1}). Complete conversion of triglyceride was observed at H_2/feed ratios >500 NL_{gas}/L_{liquid}, at 420 °C. At lower temperatures (360 °C), H_2/feed ratio considerably effected the conversion of triglycerides, with approximately 28% reduction in conversion on decreasing H_2/feed ratio from 2500 NL_{gas}/L_{liquid} to 500 NL_{gas}/L_{liquid} (Table 1). Increase in the formation of >C18 product was observed on increasing the H_2/feed ratio from 500 NL_{gas}/L_{liquid} to 2500 NL_{gas}/L_{liquid} at both 360 °C and 420 °C. The yield of >C18 products increased 1.5–1.7 times on increasing the H_2/feed ratio from 500 to 2500 NL_{gas}/L_{liquid}. This increase in the yield of >C18 product may be partly attributed to the acidic characteristics of the catalytic SiO_2–Al_2O_3 support because, such a trend was not observed over non-acidic Al_2O_3 system [30]. The increase of >C18 product yield on increasing H_2/feed ratio from 500 to 1500 NL_{gas}/L_{liquid} was more as compared to the increase from 1500 to 2500 NL_{gas}/L_{liquid} (Table 1). Correspondingly, an increase in the yield of cracked products (<C9 and C9–C14) was also observed on increasing the H_2/feed ratio. At higher temperature (420 °C), both naphtha (<C9) and kerosene (C9–C14) yields increased from 3 to 9% and 11 to 14% respectively, with increase in the H_2/feed ratio. The above observation indicated an increase in cracking reactions, which probably in turn also promoted C—C coupling reactions leading to formation of >C18 products (Table 1). These observations may be correlated with the increased cracking ability of the hydrocracking Ni–W/SiO_2–Al_2O_3 catalyst, at increased partial pressures of hydrogen and higher superficial velocities (at higher H_2/Feed ratios). Moreover there is also a decrease in yield of C15–C18 fraction from 77% at 500 H_2/Feed to 64% at 2500 H_2/Feed (Table 1) which very well correlates with the above results at higher temperatures (420 °C). At lower temperature (360 °C) increased yields of C15–C18 product is due to increased conversion of triglycerides (Table 1).

To know the combined effect of process parameters over kerosene yield, response surface plots were drawn (Fig. 7), which indicated a very strong interaction of temperature and pressure over the yield of kerosene range hydrocarbons (Fig. 7a). The inclined contours (Fig. 7a and b) to the axis indicated very strong combined influence of temperature and space velocity and pressure on kerosene range hydrocarbons. Increase in kerosene yield was favoured on increasing temperatures from 340 to 420 °C, increasing pressure from 20 to 80 bar and reducing space velocities from 12 to 1 h^{-1}. Combined interactions of pressure, H_2/Feed ratio and temperature over the kerosene range hydrocarbons was also studied (Fig. 7c and d). A very strong interaction as in case of space velocity and temperature was not observed in case of H_2/feed ratios. Parallel contours to the H_2/feed axis in both Fig. 7c and d indicated negligible influence of H_2/feed on the yield of kerosene range hydrocarbons.

The reaction trends at various conditions show that the product patterns for hydroprocessing of jatropha oil, over a hydrocracking Ni–W/SiO_2–Al_2O_3 catalyst, were drastically affected by the processing conditions and the optimum operating conditions were product specific. When naphtha and kerosene were desired products then H_2/feed ratio of 2500 NL_{gas}/L_{liquid}, space velocity approximately 1–2 h^{-1}, pressure approximately 60–80 bar and temperatures >400 °C were desirable to achieve substantial cracking. For diesel range hydrocarbons (C15–C18 and >C18), lower temperatures (370–380 °C) and lower H_2/feed ratio (1000 NL_{gas}/L_{liquid}) would reduce cracking, maximize the desired diesel product yield; further, 60–80 bar pressure with 1–2 h^{-1} space velocities resulted in complete conversion of triglycerides. Lower pressures (<60 bar) lead to cleavage of C—C bond, which formed lower carbon

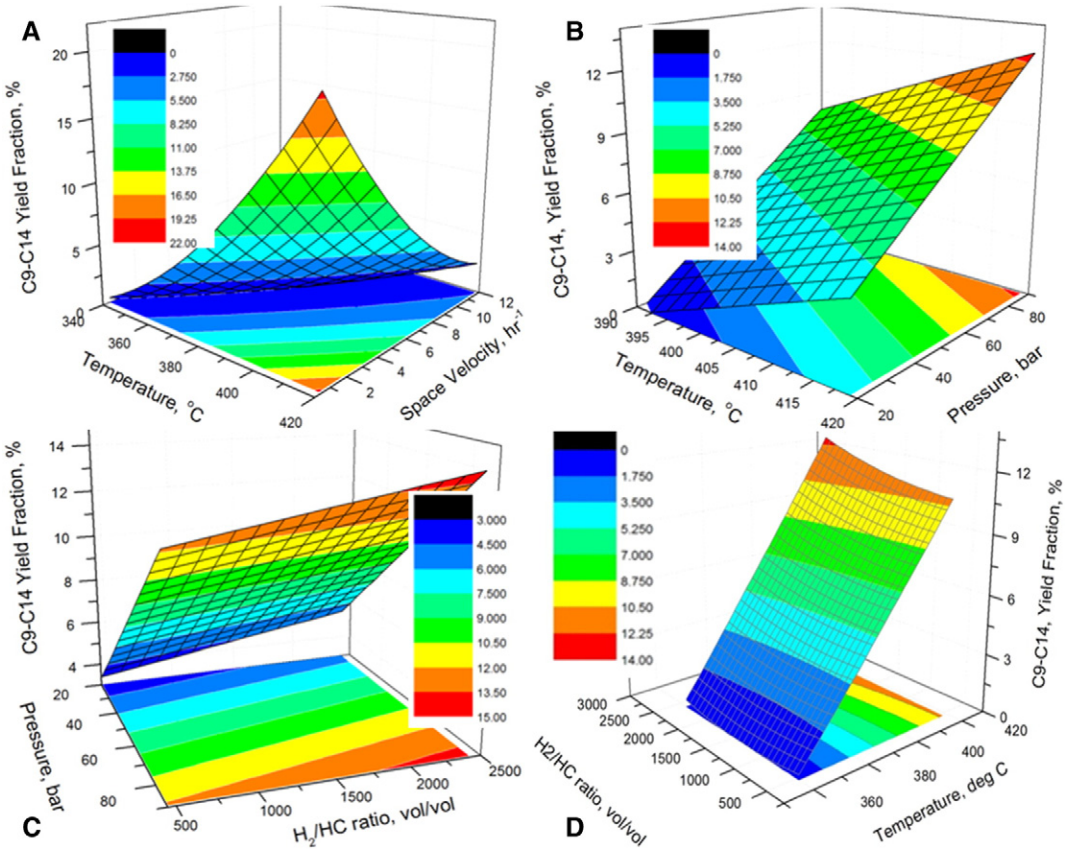

Fig. 7. Kerosene yield as a combined interaction of process parameters (A. 80 bar, 1500 NL_{gas}/L_{liquid}; B. 3 h^{-1}, 1500 NL_{gas}/L_{liquid}; C. 3 h^{-1}, 420 °C; D. 80 bar, 3 h^{-1}).

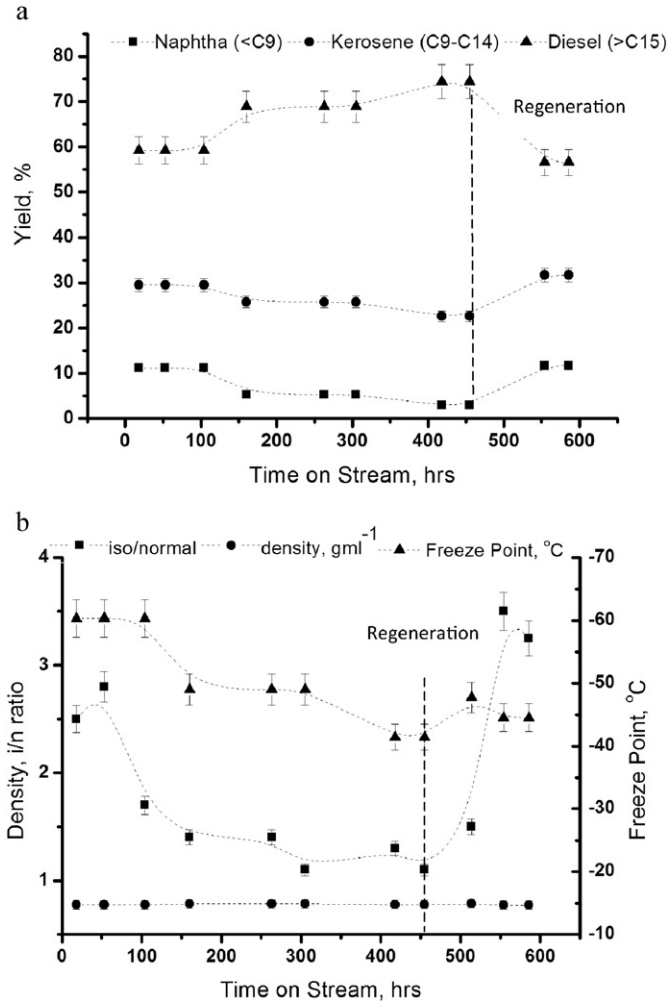

Fig. 8. Catalyst performance as a function of time on stream (a yield % of different fractionation cuts, b. iso/normal, ratio of isomers and normal hydrocarbons; density, g/ml; freeze point, °C; of kerosene (130–260 °C) fraction) (1 h^{-1}, 420 °C, 80 bar, 2500 NL_{gas}/L_{liquid}).

range (<C16) oxygenated species, identified as esters, whose concentration grew on reducing the pressures to 20 bar.

3.3. Catalyst life time and pilot plant study

Continuous pilot plant studies were conducted at 420 °C, 1 h^{-1}, 2500 NL_{gas}/L_{liquid} and 80 bar. After separation of hydrocarbon layer and water, the products were fractionated into naphtha (IBP-130 °C), kerosene (130–260 °C) and diesel (260-FBP) range cuts. Initial boiling point (IBP) of 32 °C and final boiling point (FBP) of 331 °C was observed. Final boiling point (FBP) for kerosene range was 260 °C, to meet the freeze point specifications for aviation kerosene. A constant yield of 12% naphtha (<C9), 30% kerosene (C9–C14) and 60% diesel (>C15) was obtained until 100 h of continuous operation (Fig. 8a). The yield of naphtha and kerosene decreased to 5 and 25% respectively, and the yield of diesel increased to 70%, until 480 h of operation (Fig. 8a). The physicochemical properties of kerosene range were monitored with time on stream. The product met all the specifications of ASTM D1655 for aviation kerosene Jet A-1 and ASTM D7566 for renewable Jet A-1 kerosene (Table 2). The density of the aviation bio-kerosene fraction was observed to be constant (0.778 g/ml) until 480 h of continuous operation (Fig. 8b). Commercially produced bio-aviation fuel does not have aromatics and also the density is less as compared to that obtained by the present process. The feedstock, for production of bio-aviation kerosene, is hydrodeoxygenated over a catalyst in the first stage reactor to produces saturated paraffins, which is then sent to a secondary reactor unit after separation of H_2O for isomerization/cracking reactions, to produce paraffins and isoparaffins in kerosene range. In the present work, all the reactions, i.e. isomerization, cracking, hydrotreating are targeted simultaneously in a single reactor catalyst bed with a catalyst having strong hydrogenation/dehydrogenation ability along with tailored acidity for these reactions [1,25,31]. The unsaturations in the hydrocarbon chains of triglycerides drive cyclization and condensation reactions, under acidic reaction conditions [36,37], further dehydrogenation (at sulfided metal sites) produces aromatics over this multifunctional catalyst system. High exothermicities observed during these simultaneously occurring reactions in a single reactor [38] may also be one of the reasons for the production of aromatics and naphthenes in the present process.

On evaluating the product properties, after an initial increase in isomer to normal hydrocarbon (i/n) ratio (2.8 at 50 h), it was observed to

Table 2
Detailed analysis results as per ASTM D1655/ASTM D 7566 [34], of renewable kerosene.

Test properties as per ASTM D1655/D7566	Method	Limits	Values	Error, ±
Acidity, total mg KOH/g	D 3242	0.1 (max)	0.022	0.01
Aromatics, vol%	D 1319	25 (max)	11.3	0.5
Naphthalenes, vol, %	D 1840	3 (max)	2.03	0.04
Smoke point, mm	D 1322	18 (min)	25	0.5
Sulfur, mercaptan, C mass %	D 3227	0.003 (max)	0.0004	0.0001
Sulfur, total mass %	D 4294	0.03 (max)	0.0009	0.00005
Distillation temperature, °C:	D 86D		138.7	
10% recovered, °C		205 (max)	166.4	1.0
50% recovered, °C		Report	198.2	
90% recovered, °C		Report	244.9	
Final boiling point, °C		300 (max)	260	1.0
Distillation residue, %		1.5 (max)	0.8	0.1
Distillation loss, %		1.5 (max)	0.2	0.1
Flash point, °C	D 3828F	38 (min)	45.9	0.75
Density at 15 °C, kg/m^3	D 4052	775–840	781.34	0.2
Freezing point, °C	D 5972	−47 (max)	−49.3	0.5
Viscosity −20 °C, mm^2/s	D 445	8 (max)	3.78	0.02
Net heat of combustion, MJ/kg	D 4529	42.8 (min)	43.3	0.05
THERMAL STABILITY, JFTOT	D 3241	25 (max)	3.6	
Filter pressure drop, mm Hg				
Tube deposits less than		3 (max)	2	0.1
Existent gum, mg/100 ml	D 381	7 (max)	6.2	0.2

be constant at 1.5 which reduced to 1 at 480 h, correspondingly the freeze point increased from an initial value of −60 °C to −40 °C (Fig. 8b). Due to reduced i/n ratio and freeze point of the kerosene cut in-situ regeneration using controlled concentration of N_2 and O_2 was carried out, so as to regain the catalyst activity. The catalyst activity was regained with 32% kerosene and 12% naphtha observed until 580 h of continuous operation. The i/n ratio and freeze point were also regained (Fig. 8b). This indicated that the loss in catalytic activity was not permanent and could be regained back after regeneration. Considerable localized metal deposits were observed over the used catalyst (Fe 12%, Na 2%, Mg 11%, Ca 4%, P 15%) (from SEM-EDX analysis), which were present in the jatropha oil used in the process, over a period of 600 h. These are permanent poisons which block the active sites, and cannot be removed by in-situ regenerations. To increase catalyst life time and improve the process economics, it is necessary to pre-treat the feedstock and to use appropriate guard beds at the top of the reactor, to avoid the metal deposition on the catalyst bed.

4. Conclusions

Triglyceride conversion over Ni–W catalyst system was strongly dependent on the temperature, space velocity and hydrogen partial pressures. The yield of cracked products (naphtha and kerosene) increased at higher temperatures (420 °C), higher pressures (>60 bar), optimal H_2/feed ratio (1500 NL_{gas}/L_{liquid}) and lower space velocities (0.5–2 h^{-1}). Naphtha, a lower value product, is increased at the expense of diesel yield, when targeting jet fuel as a primary product. At higher partial pressures of hydrogen (>60 bar), C—O bond cleavage leading to deoxygenation reactions were favoured, whereas at lower pressures (<60 bar) C—C bond breaking, leading to formation of oxygenated intermediates such as lower range esters and acids were more significant. Continuous pilot plant tests indicated reduction in isomerization selectivity and freeze point of aviation bio-kerosene fraction, along with marginal decrease in yield (until 480 h), which could be regained by regeneration of the catalyst active sites. The aviation bio-kerosene obtained by hydrocracking of jatropha over Ni–W/SiO_2–Al_2O_3 catalyst system meets all ASTM D7566 specifications.

Acknowledgment

The authors thank ASD, CSIR-IIP for analytical services and T. Khan and P. Alam for technical support for catalytic evaluations. MGS acknowledges UGC, India for fellowship. This work was carried under 'CSC-117' program of CSIR, India. DST, India (ICRD08-054) is acknowledged for partial research funding.

References

[1] R. Kumar, B.S. Rana, R. Tiwari, D. Verma, R. Kumar, R.K. Joshi, M.O. Garg, A.K. Sinha, Green Chem. 12 (2010) 2232–2239.
[2] R. Tiwari, B.S. Rana, R. Kumar, D. Verma, R. Kumar, R.K. Joshi, M.O. Garg, A.K. Sinha, Catal. Commun. 12 (2011) 559–562.
[3] D.S. Lee, D.W. Fahey, P.M. Forster, P.J. Newton, R.C.N. Wit, L.L. Lim, B. Owen, R. Sausen, Atmos. Environ. 43 (2009) 3520–3537.
[4] S. Bezergianni, A. Kalogianni, Bioresour. Technol. 100 (2009) 3927–3932.
[5] M. Stocker, Angew. Chem. Int. Ed. 47 (2008) 9200–9211.
[6] J.O. Metzger, Angew. Chem. Int. Ed. 45 (2006) 696–698.
[7] G.W. Huber, A. Corma, Angew. Chem. Int. Ed. 46 (2007) 7184–7201.
[8] Y. Liu, R. Sotelo-Boyas, K. Murata, T. Minowa, K. Sakanishil, Chem. Lett. 38 (2009) 552–553.
[9] A.L. Mascarelli, Nature 461 (2009) 460–461.
[10] A.A. Lappas, S. Bezergianni, I.A. Vasalos, Catal. Today 145 (2009) 55–62.
[11] S. Bezergianni, A. Kalogianni, I.A. Vasalos, Bioresour. Technol. 100 (2009) 3036–3042.
[12] S. Bezergianni, S. Voutetakis, A. Kalogianni, Ind. Eng. Chem. Res. 48 (2009) 8402–8406.
[13] S. Melis, S. Mayo, B. Leliveld, Biofuels Technol. 1 (2009) 43–47.
[14] P. Šimácek, D. Kubicka, G. Šebor, M. Pospíšil, Fuel 88 (2009) 456–460.
[15] G.W. Huber, P.O. Connor, A. Corma, Appl. Catal. A Gen. 329 (2007) 120–129.
[16] B. Donnis, R.G. Egeberg, P. Blom, K.G. Knudsen, Top. Catal. 52 (2009) 229–240.
[17] D. Kubicka, P. Simacek, N. Zilkova, Top. Catal. 52 (2009) 161–168.
[18] S. Blakey, L. Rye, C.W. Wilson, Proc. Combust. Inst. 33 (2011) 2863–2885.
[19] P. Nair, A. Bozzano, T. Kalnes, Hydrocarb. Process. (2007) (sep, 67l UOP/Eni).
[20] L. Boda, G. Onyestyak, H. Solt, F. Lonyi, J. Valyon, A. Thernesz, Appl. Catal. A Gen. 374 (2010) 158–169.
[21] S. Lestari, P. Maki-Arvela, H. Bernas, O. Simakova, R. Sjoholm, J. Beltramini, G.Q.M. Lu, J. Myllyoja, I. Simakova, D.Y. Murzin, Energy Fuel 23 (2009) 3842–3845.
[22] M. Snare, I. Kubickova, P. Maki-Arvela, K. Eranen, D.Y. Murzin, Ind. Eng. Chem. Res. 45 (2006) 5708–5715.
[23] B. Rozmyslowicz, P. Maki-Arvela, S. Lestari, O.A. Simakova, K. Eranen, I.L. Simakova, D.Y. Murzin, T.O. Salmi, Top. Catal. 53 (2010) 1274–1277.
[24] K. Murata, Y. Liu, M. Inaba, I. Takahara, Energy Fuel 24 (2010) 2404–2409.
[25] D. Verma, R. Kumar, B.S. Rana, A.K. Sinha, Energy Environ. Sci. 4 (2011) 1667–1671.
[26] J. Hancsok, T. Kasza, S. Kovacs, P. Solymosi, A. Hollo, J. Clean. Prod. 34 (2012) 76–81.
[27] J. Mikulec, J. Cvengroš, L. Joríková, M. Banič, A. Kleinová, J. Clean. Prod. 18 (2010) 917–926.
[28] M. Krár, S. Kovács, D. Kalló, J. Hancsók, Bioresour. Technol. 101 (2010) 9287–9293.
[29] T. Morgan, D. Grubb, E.S. Jimenez, M. Crocker, Top. Catal. 53 (2010) 820–829.
[30] M. Anand, A.K. Sinha, Bioresour. Technol. 126 (2012) 148–155.
[31] A.K. Sinha, M. Anand, B.S. Rana, R. Kumar, S.A. Farooqui, M.G. Sibi, R. Kumar, R.K. Joshi, Catal. Surv. Jpn. 17 (1) (2013) 1–13.
[32] G. Bergeret, P. Gallezot, Particle size and dispersion measurements, Handbook of Heterogeneous Catalysis 2008, pp. 738–765.
[33] P.J. Mangnus, A. Riezebos, A.D.V. Langeveld, J.A. Moulijn, J. Catal. 151 (1995) 178–191.
[34] Standard Specification for Aviation Turbine Fuel Containing Synthesized Hydrocarbons, 2016, http://dx.doi.org/10.1520/D7566-16.
[35] J. Liu, C. Liu, G. Zhou, S. Shen, L. Rong, Green Chem. 14 (2012) 2499–2505.
[36] D. Verma, B.S. Rana, R. Kumar, M.G. Sibi, A.K. Sinha, Appl. Catal. A Gen. 490 (2015) 108–116.
[37] M. Anand, M.G. Sibi, D. Verma, A.K.J. Sinha, Chem. Sci. 126 (2) (2014) 473–480.
[38] M. Anand, S.A. Farooqui, R. Kumar, R. Joshi, R. Kumar, M.G. Sibi, H. Singh, A.K. Sinha, Appl. Catal. A Gen. 516 (2016) 144–152.